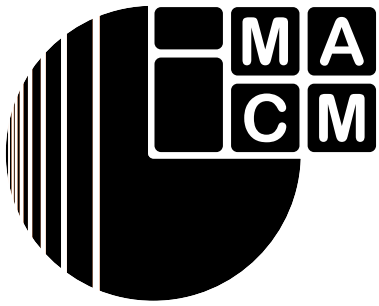

Bergische Universität Wuppertal

Fachbereich Mathematik und Naturwissenschaften

Institute of Mathematical Modelling, Analysis and Computational Mathematics (IMACM)

Preprint BUW-IMACM 19/15

Andrey G. Tyshchenko, Pavel S. Petrov and Matthias Ehrhardt

Wide-angle mode parabolic equation with transparent boundary conditions and its applications in shallow water acoustics

May 2019

http://www.math.uni-wuppertal.de

Wide-angle mode parabolic equation with transparent boundary conditions and its applications in shallow water acoustics

Andrey G. Tyshchenko, Pavel S. Petrov
V.I.Il'ichev Pacific Oceanological Institute, 43 Baltiyskaya St., Vladivostok, 690041, Russia
Far Eastern Federal University, 8 Sukhanova St., 690950, Vladivostok, Russia;
e-mail: ggoldenfeniks@gmail.com, petrov@poi.dvo.ru

Matthias Ehrhardt
Bergische Universität Wuppertal, Gaußstrasse 20, D-42119 Wuppertal, Germany;
e-mail: ehrhardt@uni-wuppertal.de

A wide-angle mode parabolic equation is obtained from the horizontal refraction equation by using the rational-linear approximation of the square-root operator. A finite-difference scheme for the numerical solution of the derived equation is developed. The scheme is based on standard Crank-Nicolson method and fully-discrete transparent boundary conditions that allow for an accurate simulation of sound propagation on an unbounded domain.

1 Introduction

The representation of an acoustic field in a 3D shallow-water waveguide in the form of a modal decomposition leads to 2D Helmholtz-type equations for the modal amplitudes [1, 2, 3] (see Eq. (2) below). They are often called *horizontal refraction equations* (HREs). Many techniques were developed for the solution of HREs since they appeared in literature in 1970s for the first time, including ray theory [2], parabolic approximation [4] and a variety of analytical methods (see, e.g., [3]).

Parabolic approximations to HREs also known as *mode parabolic equations* (MPEs) were first introduced in ocean acoustics 1993 by Collins [4]. In principle, they can be solved numerically by exactly the same methods as Schrödinger equations and (paraxial) parabolic equations from optics and radiophysics (e.g., by finite differences, exponential time differencing, split-step Fourier and many other methods [1]). In some important cases MPEs also admit analytical solutions by group-theoretical approaches [5, 6].

To our knowledge, until now little attention was paid in literature to the derivation, validation and numerical solution of *wide-angle mode parabolic equations* (WAMPEs), although standard wide-angle parabolic equations (i.e., equations solved in vertical plane in r, z coordinates) are widely used in underwater acoustics [1, 7, 8]. In this study we derive simple rational-linear WAMPE that approximates HRE and present its numerical validation by the solution of two test problems. A finite-difference scheme of Crank-Nicolson type is developed for the numerical solution of the derived WAMPE.

An inherent feature of MPEs is that they are always solved on unbounded domains (by contrast to "normal", or "vertical" parabolic equations in underwater acoustics which are solved in a stack of layers that have ocean surface as their upper boundary and, at least in theory, some lower boundary at the sea bottom as well). Thus, an artificial truncation of the computational domain is an inevitable step of numerical solution of such equations. At artificial boundaries one has to set up transparent/absorbing boundary conditions (TBCs/ABCs). Such conditions are well-developed for narrow-angle parabolic equations [9, 10].

In our study we adapted fully-discrete TBCs from [11] (originally developed for "vertical" parabolic equations) for our numerical scheme for solving WAMPEs. The resulting computational tool produces a robust and highly accurate approximation to the solution of the HRE.

2 The Horizontal Refraction Equation

The sound field $p(x, y, z)$ produced by a time-harmonic point source in a 3D shallow-water waveguide is described by the three-dimensional Helmholtz equation (where z denotes the depth, and x, y are the horizontal coordinates). Its solution can be expressed in the form of modal de-

composition [1, 3]

$$p(x,y,z)=\sum_{j=1}^{J}A_j(x,y)\varphi_j(z,x,y), \qquad (1)$$

where $\varphi_j(z,x,y)$ are the modal functions [1] and $A_j(x,y)$ are the modal amplitudes, which satisfy the so-called horizontal refraction equation [1, 2]:

$$\frac{\partial^2 A_j}{\partial x^2}+\frac{\partial^2 A_j}{\partial y^2}+k_j^2(x,y)A_j=-\varphi_j(z_s)\delta(x)\delta(y), \quad (2)$$

where $k_j=k_j(x,y)$ are modal wavenumbers, and z_s is the source depth. Modal functions $\varphi_j(z,x,y)$ and the respective horizontal wavenumbers $k_j(x,y)$ can be obtained from an acoustical spectral problem (see [1] for the details).

3 Wide-Angle Mode Parabolic Equation

In this section we obtain a wide-angle mode parabolic equation from the HRE (2). To do so, we first factorize (2) as

$$\left(\partial_x+i\sqrt{k_j^2+\partial_z^2}\right)\left(\partial_x-i\sqrt{k_j^2+\partial_z^2}\right)A_j=0 \quad (3)$$

and separate its solution consisting of the waves propagating in the positive direction of the x axis

$$\left(\partial_x-i\sqrt{k_j^2+\partial_z^2}\right)A_j=0\,. \qquad (4)$$

Introducing the modal reference wavenumber $k_{j,0}$ and extracting the principal oscillation from A_j

$$A_j(x,y)=e^{ik_{j,0}x}\mathcal{A}_j(x,y)\,,$$

we obtain the pseudo-differential mode parabolic equation

$$\frac{\partial\mathcal{A}_j}{\partial x}=ik_{j,0}\left(\sqrt{1+L_j}-1\right)\mathcal{A}_j\,, \qquad (5)$$

where $k_{j,0}L_j=\partial_y^2+k_j^2-k_{j,0}^2$. Next we formally approximate the square-root operator $\sqrt{1+L_j}$ by a rational-linear function

$$\sqrt{1+L_j}\approx\frac{a+bL_j}{1+cL_j}\,, \qquad (6)$$

where a,b,c are certain constants chosen as explained in [1]. Finally, substituting (6) into (5) and denoting $\alpha_0=a-1$, $\alpha_1=b-c$, we obtain the following WAMPE

$$\frac{\partial\mathcal{A}_j}{\partial x}=ik_{j,0}\frac{\alpha_0+\alpha_1L_j}{1+cL_j}\mathcal{A}_j\,. \qquad (7)$$

For the initial condition for (7) at $x=0$ we use the so-called PE starter from Greene's source [1, 8] that can be written as

$$\mathcal{A}_j(0,y)=\frac{\varphi_j(z_s)}{2\sqrt{\pi}}\left(1.4467-0.8402k_{j,0}^2y^2\right)e^{-\frac{k_{j,0}^2y^2}{1.5256}}\,. \quad (8)$$

4 The Numerical Scheme

Here we derive a numerical scheme for solving (7) based on the standard CrankNicolson discretization. Let us consider a uniform grid

$$\begin{aligned} x_n&=n\Delta x, & n&=\overline{0,N}\,,\\ y_m&=y_0+m\Delta y, & m&=\overline{0,M}\,,\\ k_j^{n,m}&=k_j(x_n,y_m)\,,\\ \mathcal{A}_j^{n,m}&\approx\mathcal{A}_j(x_n,y_m)\,. \end{aligned} \qquad (9)$$

First we rewrite Eq. (7) as

$$(1+cL_j)\frac{\partial\mathcal{A}_j}{\partial x}=ik_{j,0}(\alpha_0+\alpha_1L_j)\mathcal{A}_j\,, \qquad (10)$$

and use Crank-Nicolson discretization to obtain the following finite difference equation:

$$\left(1+cL_j^{\frac{n}{2},m}\right)\frac{\mathcal{A}_j^{n+1,m}-\mathcal{A}_j^{n,m}}{\Delta x}= ik_{j,0}\left(\alpha_0+\alpha_1L_j^{\frac{n}{2},m}\right)\frac{\mathcal{A}_j^{n+1,m}+\mathcal{A}_j^{n,m}}{2}\,, \quad (11)$$

where

$$k_{j,0}^2L_j^{\frac{n}{2},m}=\partial_y^2+\kappa_j^{\frac{n}{2},m}-k_{j,0}^2\,,$$
$$\kappa_j^{\frac{n}{2},m}=\frac{\left(k_j^{n+1,m}\right)^2+\left(k_j^{n,m}\right)^2}{2}.$$

Collecting terms with identical n and introducing

$$\beta_{j,0}=2-\alpha_0ik_{j,0}\Delta x,\quad \beta_{j,1}=2c-\alpha_1ik_{j,0}\Delta x\,,$$
$$\gamma_{j,0}=2+\alpha_0ik_{j,0}\Delta x,\quad \gamma_{j,1}=2c+\alpha_1ik_{j,0}\Delta x\,,$$

we arrive at the marching scheme which approximates the evolution equation (10):

$$\left(\beta_{j,0}+\beta_{j,1}L_j^{\frac{n}{2},m}\right)\mathcal{A}_j^{n+1,m}= \left(\gamma_{j,0}+\gamma_{j,1}L_j^{\frac{n}{2},m}\right)\mathcal{A}_j^{n,m}\,. \quad (12)$$

Now we replace the operator $L_j^{\frac{n}{2},m}$ by its second-order finite-difference counterpart

$$\partial_y^2\mathcal{A}_j^{n,m}\approx\frac{\mathcal{A}_j^{n,m+1}-2\mathcal{A}_j^{n,m}+\mathcal{A}_j^{n,m-1}}{\Delta y^2} \qquad (13)$$

and obtain the following discretized WAMPE:

$$p_{j,0}\mathcal{A}_j^{n+1,m+1} + q_{j,0}^{n,m}\mathcal{A}_j^{n+1,m} + p_{j,0}\mathcal{A}_j^{n+1,m-1} = p_{j,1}\mathcal{A}_j^{n,m+1} + q_{j,1}^{n,m}\mathcal{A}_j^{n,m} + p_{j,1}\mathcal{A}_j^{n,m-1}\,,$$

where

$$p_{j,0} = \frac{\beta_{j,1}}{k_{j,0}^2\Delta y^2}, \quad q_{j,0}^{n,m} = \beta_{j,0} - \beta_{j,1}\mathcal{L}_j^{n,m}\,,$$
$$p_{j,1} = \frac{\gamma_{j,1}}{k_{j,0}^2\Delta y^2}, \quad q_{j,1}^{n,m} = \gamma_{j,0} - \gamma_{j,1}\mathcal{L}_j^{n,m}\,, \quad (14)$$
$$\mathcal{L}_j^{n,m} = \frac{1}{k_{j,0}^2}\left(\kappa_j^{\frac{n}{2},m} - k_{j,0}^2 - \frac{2}{\Delta y^2}\right).$$

In order to perform the numerical simulation of the propagation in an unbounded horizontal domain we use discrete *transparent boundary conditions* (TBCs) developed in [11] at $y = y_0$ and $y = y_N$.

For applying the fully-discrete TBCs [11] we must assume that k_j is constant (i.e., x-independent) at the boundaries $y = y_0$ and $y = y_N$:

$$k_j^0 = k_j\left(0, y_0\right), \quad k_j^M = k_j\left(0, y_M\right). \quad (15)$$

Indeed, if media inhomogeneities are present at the boundaries, then we cannot neglect the waves scattered back to the domain interior by these inhomogeneities.

Fully-discrete TBCs at $y = y_0$ are written as

$$(1+iq)\,\mathcal{A}_j^{n+1,1} - s_0^{(0)}\mathcal{A}_j^{n+1,0} = -\left(1-iq\right)\mathcal{A}_j^{n,1} + \sum_{l=1}^{n}\mathcal{A}_j^{l,0}s_0^{(n-l+1)} \quad (16)$$

Where $q = 2c/(k_{j,0}\alpha_1\Delta x)$. The coefficients $s_0^{(l)}$ can be calculated using the recursive formula [11]:

$$s_0^{(0)} = 1 + iq - \frac{i}{2}\left(\gamma + i\sigma + \sqrt[+]{A}\right),$$
$$s_0^{(1)} = 1 - iq + \frac{i}{2}\left(\gamma - i\sigma + \frac{B}{\sqrt[+]{A}}\right),$$
$$s_0^{(2)} = \frac{\mu}{2\lambda}\left(s_0^{(1)} + \frac{s_0^{(0)}}{\lambda\mu} - \beta\right), \quad (17)$$
$$s_0^{(n+1)} = \frac{1}{n+1}\left(\frac{2n-1}{\lambda}\mu s_0^{(n)} - \frac{n-2}{\lambda^2}s_0^{(n-1)}\right),$$

where

$$R = \frac{2k_{j,0}}{\alpha_1}\frac{\Delta y^2}{\Delta x} \qquad \delta = 1 - c\left(1 - N_0^2\right),$$
$$\kappa = \frac{\Delta x k_{j,0}}{2}\left(\alpha - \alpha_1\left(1 - N_0^2\right)\right),$$
$$\gamma = R\delta \qquad \sigma = -R\kappa \qquad N_0 = \frac{k_{j,0}}{k_j^0},$$
$$\lambda = \frac{\sqrt[+]{A}}{\sqrt[+]{C}} \qquad \mu = \frac{B}{\sqrt[+]{A}\,\sqrt[+]{C}},$$
$$A = (\gamma - i\sigma)\left(\gamma - 4q + i\left(\sigma + 4\right)\right),$$
$$B = \gamma\left(\gamma - 4q\right) + \sigma\left(\sigma + 4\right),$$
$$C = (\gamma - i\sigma)\left(\gamma - 4q - i\left(\sigma + 4\right)\right),$$
$$\beta = 1 - iq + \frac{i}{2}\left(\gamma - i\sigma\right) + \frac{C}{B}\left(1 + iq - \frac{i}{2}\left(\gamma + i\sigma\right)\right). \quad (18)$$

At $y = y_N$ the TBCs are written in the form

$$(1+iq)\,\mathcal{A}_j^{n+1,M-1} - s_M^{(0)}\mathcal{A}_j^{n+1,M} = -\left(1-iq\right)\mathcal{A}_j^{n,M-1} + \sum_{l=1}^{n}\mathcal{A}_j^{l,M}s_M^{(n-l+1)}, \quad (19)$$

where the coefficients $s_M^{(l)}$ are calculated analogously to those in Eq. (17).

5 Numerical Examples

In the following numerical examples the coefficients a, b, c in (6) are chosen from Claerbout's square-root operator approximation [1]:

$$\sqrt{1+L_j} \approx \frac{1 + 0.75L_j}{1 + 0.25L_j}. \quad (20)$$

The mode functions $\varphi_j(z, x, y)$ and the respective wavenumbers $k_j(x, y)$ are obtained by solving acoustical spectral problem using the finite-difference method [1].

5.1 Shallow-Water Waveguide with Flat Bottom

We start with the validation of the derived numerical scheme by simulating the propagation of acoustic waves in the Pekeris waveguide (i.e., the water depth is constant), for which the analytical solution can be written as [1]

$$p(x,y,z) = \frac{i}{4}\sum_{j=1}^{\infty}\varphi_j(z_s)\varphi_j(z)\,H_0^{(1)}\left(k_j\sqrt{x^2+y^2}\right), \quad (21)$$

where $H_0^{(1)}$ denotes the zeroth-order Hankel function of the first kind. In this example the point source is located at $x = y = 0$, $z_s = 100\,\text{m}$, the water depth is 200 m, the acoustic field is computed at depth $z = 30\,\text{m}$ on the uniform grid:

$$\begin{aligned} y_0 &= -4\,\text{km}, \quad & y_1 &= 4\,\text{km}, \quad & M &= 8001\,, \\ & & x_1 &= 10\,\text{km}, \quad & N &= 10001\,. \end{aligned} \tag{22}$$

The computational results are shown in Fig. 1. From this figure it is clear that in general our numerical scheme approximates accurately the analytical solution, although some numerical noise is present in the vicinity of the source (also note that despite being wide-angle, our MPE still has a limited aperture in the horizontal plane).

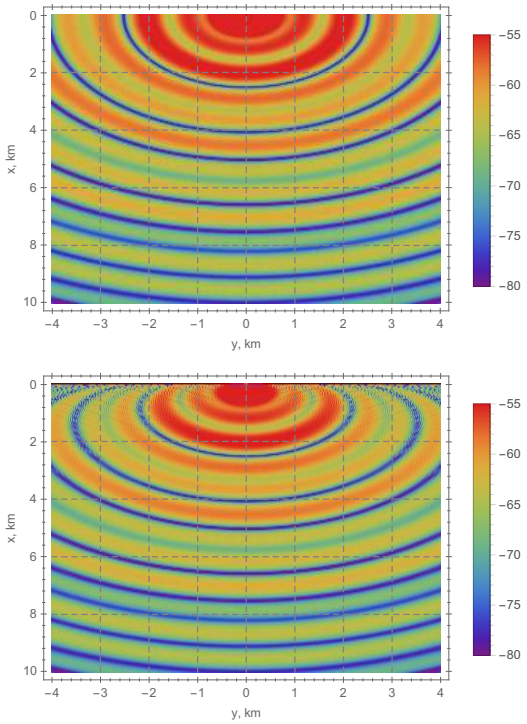

Figure 1: Acoustic field (in dB re 1 m) at the depth $z = 30\,\text{m}$ computed by the analytical formula (21) (top) and by the numerical solution of the WAMPE (bottom).

5.2 *Shallow Sea with Underwater Canyon*

In the second example we consider the propagation of the acoustic waves produced by a point source in a shallow sea with an underwater canyon (see schematic in Fig. 2). The bottom relief is described

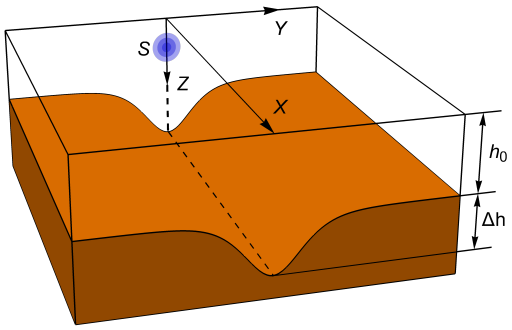

Figure 2: Schematic illustration of an underwater canyon.

by the formula

$$z = h(y) = h_0 + \Delta h \sec(\sigma y). \tag{23}$$

A point source S is located at $x = y = 0$, $z = z_s$. In this example we compute the acoustic field at the depth $z = z_s$ and consider the following parameters (Fig. 3)

$$\begin{aligned} h_0 &= 50\,\text{m}, \quad & \Delta h &= 5\,\text{m}, \quad & \sigma &= 0.005\,, \\ z_s &= 10\,\text{m}, \quad & x_1 &= 30\,\text{km}, \quad & N &= 30001\,, \\ y_0 &= -1\,\text{km}, \quad & y_1 &= 1\,\text{km}, \quad & M &= 2001\,. \end{aligned} \tag{24}$$

The WAMPE solution is compared with the solution of the narrow angle adiabatic MPE [1, 5]. As shown in Fig. 4 the solutions are identical and therefore the numerical scheme is well-suited for sound propagation in a shallow-water waveguide with bottom inhomogeneities. This result also shows that in fact the aperture of the narrow-angle MPE is sufficient for accurately handling this problem. However, in the general case the narrow-angle MPE is known to be insufficiently accurate, as the horizontal rays refracted by the bottom may travel at larger angles than can be taken into account by the standard approximation. Such cases will be considered in future work, while in this study we restrict our attention to the validation of the developed computational tool.

6 Conclusion

In this study a simple rational-linear wide-angle MPE was derived. A numerical scheme of Crank-Nicolson type with fully-discrete TBCs was proposed for the derived WAMPE. The resulting numerical model can accurately handle 3D shallow-water sound propagation problems. The three-dimensional effects are taken into account via the

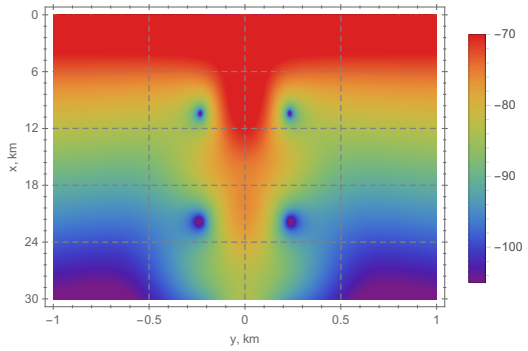

Figure 3: Acoustic field in a shallow-water see with underwater canyon $p\,(x, y, z = z_s)$ in dB re 1 m.

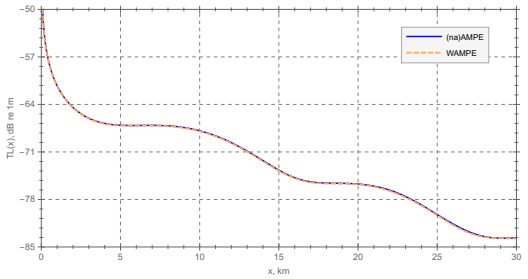

Figure 4: Transmission loss (in dB re 1 m) along the y axis.

dependence of the modal eigenvalues $k_j = k_j(x, y)$ on the horizontal coordinates x, y. Mode coupling effects are not taken into account in this model, and a coupled mode wide-angle MPE will be developed in future work.

Acknowledgements

This study was supported by the Russian Foundation for Basic Research under the contracts No. 18-05-00057_a and No. 18-35-20081_mol_a_ved. A.T. and P.P. were also partly supported by the POI FEBRAS Program "Mathematical simulation and analysis of dynamical processes in the ocean" (No. 0271-2019-0001). P.P. was also partly supported by the Heinrich Hertz Stiftung.

References

[1] F. A. Jensen, W. Kuperman, M. Porter, and H. Schmidt, 2011, *Computational Ocean Acoustics*, Springer, New-York.

[2] R. Burridge and H. Weinberg, 1977, Horizontal rays and vertical modes, *in: Wave propagation and underwater acoustics*. Springer, pp. 86–152.

[3] P. S. Petrov and T. N. Petrova, 2014, Asymptotic solution for the problem of sound propagation in a sea with an underwater canyon, *J. Acoust. Soc. Am.*, Vol. **136**, pp. EL281EL287, 2014.

[4] M. D. Collins, 1993, The adiabatic mode parabolic equation, *J. Acoust. Soc. Am.*, Vol. **94**, pp. 2269–2278.

[5] P. S. Petrov, F. Sturm, 2016, An explicit analytical solution for sound propagation in a three-dimensional penetrable wedge with small apex angle, *J. Acoust. Soc. Am*, Vol. **139**, pp. 1343–1352

[6] P. S. Petrov, S. V. Prants and T. N. Petrova, 2017, Analytical lie-algebraic solution of a 3D sound propagation problem in the ocean, *Physics Letters A*, Vol. 381, pp. 1921–1925.

[7] J. F. Claerbout, 1985, *Fundamentals of Geophysical Data Processing*, Blackwell, Oxford.

[8] R. R. Greene, 1984, The rational approximation to the acoustic wave equation with bottom interaction, *J. Acoust. Soc. Am*, Vol. **76**, pp. 1764–1773.

[9] V. A. Baskakov, A. V. Popov, 1991, Implementation of transparent boundaries for numerical solution of the Schrödinger equation, *Wave Motion*, **vol. 14**, pp. 123–128.

[10] X. Antoine, A. Arnold, C. Besse, M. Ehrhardt, A. Schädle, 2008, A review of transparent and artificial boundary condition techniques for linear and nonlinear Schrödinger equations, *Commun. Comp. Phys.*, **vol. 4**, pp. 729–796.

[11] A. Arnold, M. Ehrhardt, 1998, Discrete transparent boundary conditions for wide angle parabolic equations in underwater acoustics, *J. Comp. Phys*, Vol. **145**, pp. 611–638